

Limonoids from *Aphanamixis polystachya* and Their Antifeedant Activity

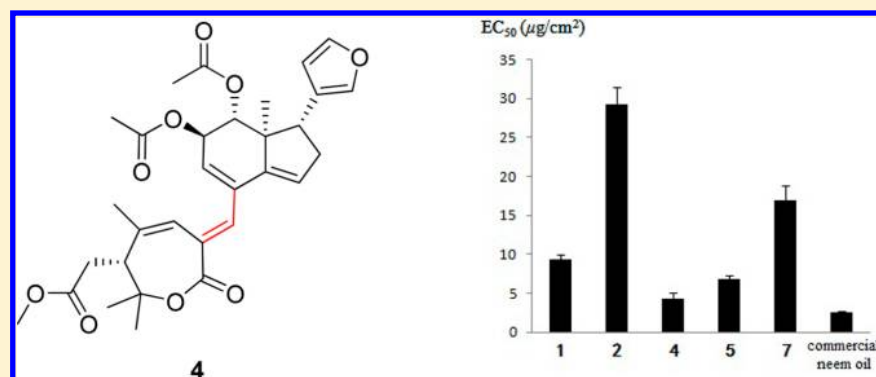
Jie-Yun Cai,^{†,‡} Duo-Zhi Chen,[†] Shi-Hong Luo,[†] Ning-Chuan Kong,[†] Yu Zhang,[†] Ying-Tong Di,[†] Qiang Zhang,[§] Juan Hua,[†] Shu-Xi Jing,[†] Shun-Lin Li,[†] Sheng-Hong Li,^{*,†} Xiao-Jiang Hao,^{*,†} and Hong-Ping He^{*,†}

[†]State Key Laboratory of Phytochemistry and Plant Resources in West China, Kunming Institute of Botany, Chinese Academy of Sciences, Kunming 650201, Yunnan, People's Republic of China

[‡]Yunnan Institute of Tobacco Quality Inspection & Supervision, Kunming 650106, Yunnan, People's Republic of China

[§]Northwest Agriculture and Forestry University, Yangling 712100, Shaanxi, People's Republic of China

S Supporting Information



ABSTRACT: Eight new aphanamixoid-type aphanamixoids (C–J, 1–8) and six new prieurianin-type limonoids, aphanamixoids K–P (9–14), along with 10 known terpenoids were isolated from *Aphanamixis polystachya*, and their structures were established by spectroscopic data analysis. Among the new limonoids, 13 compounds exhibited antifeedant activity against the generalist *Helicoverpa armigera*, a plant-feeding insect, at various concentration levels. In particular, compounds 1, 4, and 5 showed potent activities with EC_{50} values of 0.017, 0.008, and 0.012 $\mu\text{mol}/\text{cm}^2$, respectively. On the basis of a preliminary structure–activity relationship analysis, some potential active sites in the aphanamixoid-type limonoid molecules are proposed.

Studies on insect pest control measures for crops are important for the development of global agriculture. Traditional pesticides are often damaging to the environment and pose a threat to human health.¹ Consequently, a large number of studies examining the use of biopesticides have been reported. Many studies have implied that limonoids, which are structurally diverse, highly oxygenated, and highly bioactive tetranortriterpenoids, could be ideal candidates as natural insect antifeedants.²

Previous chemical studies on the plant *Aphanamixis polystachya* (Wall.) R. N. Parker (Meliaceae) have revealed that limonoids are major secondary metabolites of this species and have led to the discovery of several substances with novel carbon skeletons, such as aphanamolide A,³ aphapolynin A,⁴ and aphanamixoid A,⁵ as well as many new structures with various bioactivities.⁶

Herein, 14 new limonoids are reported, including eight aphanamixoid-type and six prieurianin-type limonoids isolated from *A. polystachya*, together with 10 other known terpenoids. The new limonoids were established by spectroscopic analysis and by using the electronic circular dichroism (ECD) exciton

chirality method. The aphanamixoid-type limonoids, a novel class of limonoids derived from prieurianin-type limonoids, are characterized by the cleavage of the bond between C-9 and C-10 and formation of a bond between C-2 and C-30. Evaluation against *Helicoverpa armigera* has shown that the aphanamixoids exhibit potent antifeedant activity. In addition, preliminary structure–activity relationship studies of the aphanamixoids have indicated that the olefinic bond, the $\Delta^{2,30}$ configuration, and the substituent at C-12 all affect the resultant antifeedant potency significantly. Taken together, these findings suggest that aphanamixoid-type limonoids are promising candidates as novel natural pesticides.

RESULTS AND DISCUSSION

Aphanamixoid C (1) was obtained as an amorphous powder. The molecular formula $\text{C}_{31}\text{H}_{38}\text{O}_9$, representing 13 indices of

Special Issue: Special Issue in Honor of Otto Sticher

Received: August 20, 2013

Published: November 20, 2013

Table 1. ^1H and ^{13}C NMR Data for Compounds 1–3 in CDCl_3 (J in Hz)

position	1^a		2^a		3^b	
	δ_{C}	δ_{H} (mult; J , Hz)	δ_{C}	δ_{H} (mult; J , Hz)	δ_{C}	δ_{H} (mult; J , Hz)
1	119.7, CH	5.16, s	120.1, CH	5.18, s	120.0, CH	5.09, s
2	43.8, CH	3.42, br s	44.0, CH	3.44, br s	44.0, CH	3.36, br s
3	172.4, C		171.9, C		172.6, C	
4	81.6, C		81.6, C		81.9, C	
5	47.8, CH	2.76, dd (6.0, 3.5)	48.0, CH	2.76, dd (6.1, 4.1)	48.1, CH	2.69, dd (6.2, 4.2)
6a	33.9, CH_2	2.82, dd (16.9, 6.0)	34.1, CH_2	2.82, dd (16.9, 6.1)	34.7, CH_2	2.75, dd (17.0, 6.2)
6b		2.23, dd (16.9, 3.5)		2.24, dd (16.9, 4.1)		2.17, dd (17.0, 4.2)
7	173.4, C		173.3, C		173.7, C	
8	133.4, C		133.4, C		133.7, C	
9	124.16, CH	5.38, br s	124.0, CH	5.38, br s	124.3, CH	5.30, br s
10	138.2, C		137.7, C		138.3, C	
11	72.6, CH	5.57, d (8.4)	72.6, CH	5.64, d (8.4)	72.9, CH	5.53, d (8.6)
12	78.5, CH	5.28, d (8.4)	78.6, CH	5.35, d (8.4)	78.1, CH	5.22, d (8.6)
13	51.1, C		51.5, C		51.4, C	
14	146.4, C		146.6, C		146.9, C	
15	124.20, CH	5.80, br s	124.5, CH	5.80, br s	124.6, CH	5.75, br s
16	38.3, CH_2	2.60, m	38.2, CH_2	2.60, m	39.0, CH_2	2.50, m
17	45.5, CH	3.25, t (9.3)	45.5, CH	3.28, dd (10.5, 8.7)	45.8, CH	3.24, dd (10.9, 8.2)
18	14.3, CH_3	1.02, s	14.5, CH_3	1.04, s	14.6, CH_3	0.99, s
19	25.8, CH_3	1.84, s	25.9, CH_3	1.79, s	25.7, CH_3	1.72, s
20	123.8, C		123.6, C		124.1, C	
21	140.0, CH	7.21, s	140.3, CH	7.10, s	140.9, CH	7.13, s
22	111.2, CH	6.30, br s	111.1, CH	6.25, br s	111.8, CH	6.26, br s
23	142.3, CH	7.35, br s	142.0, CH	7.27, br s	142.5, CH	7.26, br s
28	28.7, CH_3	1.37, s	28.7, CH_3	1.37, s	29.0, CH_3	1.30, s
29	25.5, CH_3	1.62, s	25.4, CH_3	1.62, s	26.0, CH_3	1.56, s
30a	34.4, CH_2	3.00, dd (14.3, 3.2)	34.5, CH_2	3.01, dd (14.6, 4.5)	34.2, CH_2	2.93, dd (14.7, 4.6)
30b		2.37, dd (14.3, 9.3)		2.38, dd (14.6, 9.3)		2.31, dd (14.7, 9.6)
7-OMe	52.1, CH_3	3.70, s	52.0, CH_3	3.70, s	52.6, CH_3	3.64, s
11-O-Ac	170.90, C		170.8, C		171.4, C	
	21.1, CH_3	2.04, s	21.0, CH_3	2.00, s	21.3, CH_3	1.96, s
12-O-1'	170.88, C		167.6, C		176.2, C	
12-O-2'	21.0, CH_3	1.78, s	128.4, C		41.7, CH	2.06, m
12-O-3'			138.3, CH	6.62, q (7.1)	26.3, CH_2	1.44, m
						1.22, m
12-O-4'			14.2, CH_3	1.73, d (7.1)	12.1, CH_3	0.77, ^c m
12-O-5'			11.7, CH_3	1.63, s	16.4, CH_3	0.78, ^c m

^a ^1H NMR spectra were recorded at 400 MHz and ^{13}C NMR spectra at 100 MHz. ^b ^1H NMR spectra were recorded at 600 MHz and ^{13}C NMR spectra at 150 MHz. ^cOverlapped, signals assigned by ^1H – ^1H COSY, HSQC, and HMBC spectra without designating multiplicity.

hydrogen deficiency, was established by HREIMS ($[\text{M}]^+$, 544.2524; calcd for $\text{C}_{31}\text{H}_{38}\text{O}_9$, 544.2516) and NMR spectroscopy (Table 1). The UV absorption at 246 nm indicated the presence of conjugated double bonds. IR absorptions at 1743 and 1738 cm^{-1} , as well as ^{13}C NMR signals at δ 173.4, 172.4, 170.90, and 170.88, revealed the presence of four ester carbonyl groups. Along with a methoxy group (δ_{H} 3.70; δ_{C} 52.1) and two acetoxy groups (δ_{H} 2.04, δ_{C} 21.1, 170.9; δ_{H} 1.78, δ_{C} 21.0, 170.9), it was found that **1** contains 26 carbons, including a β -substituted furan ring (δ_{H} 6.30, 7.21, 7.35; δ_{C} 111.2, 140.0, 142.3, 123.8) and four tertiary methyl groups (δ_{H} 1.02, 1.37, 1.62, 1.84). The above data indicated that **1** is a highly oxygenated tetranortriterpenoid. The NMR spectra of **1** suggested that the four carbonyls and five olefinic bonds accounted for nine out of the 13 indices of hydrogen deficiency, which thus required the presence of four rings in the molecule.

The 1D- and 2D-NMR spectra of **1** were found to be similar to those of aphanamixoid A,⁵ a ring A,B-*seco*-limonoid with a C-2–C-30 bond, with compound **1** found to bear an additional

acetoxy group. The two acetoxy groups present in **1** were assigned at C-11 and C-12 from the relevant HMBC correlations (Figure 1). Therefore, the gross structure of **1** could be proposed.

The relative configuration of **1** was determined from the ROESY spectrum (Figure S1, Supporting Information). The ROESY correlation of H-17/H-12 indicated that H-17 and H-12 are β -oriented, whereas the correlation of H₃-18/H-11 suggested an α -orientation for both Me-18 and H-11. The ROESY correlations of H₃-29/H-2 and H-2/H-5 indicated that H-2, H-5, and Me-29 are on the same face of ring A, and these were assigned arbitrarily as being β -oriented. Furthermore, the chemical shifts of the ^1H and ^{13}C NMR spectra of compound **1** and aphanamixoid A were shown to be similar, with a deviation of ~ 0.5 ppm. The H-2 and H-5 protons of **1** were assigned as β -oriented according to the configuration of aphanamixoid A, as confirmed by X-ray crystallographic analysis and supported by a plausible biosynthetic pathway reported previously.⁵

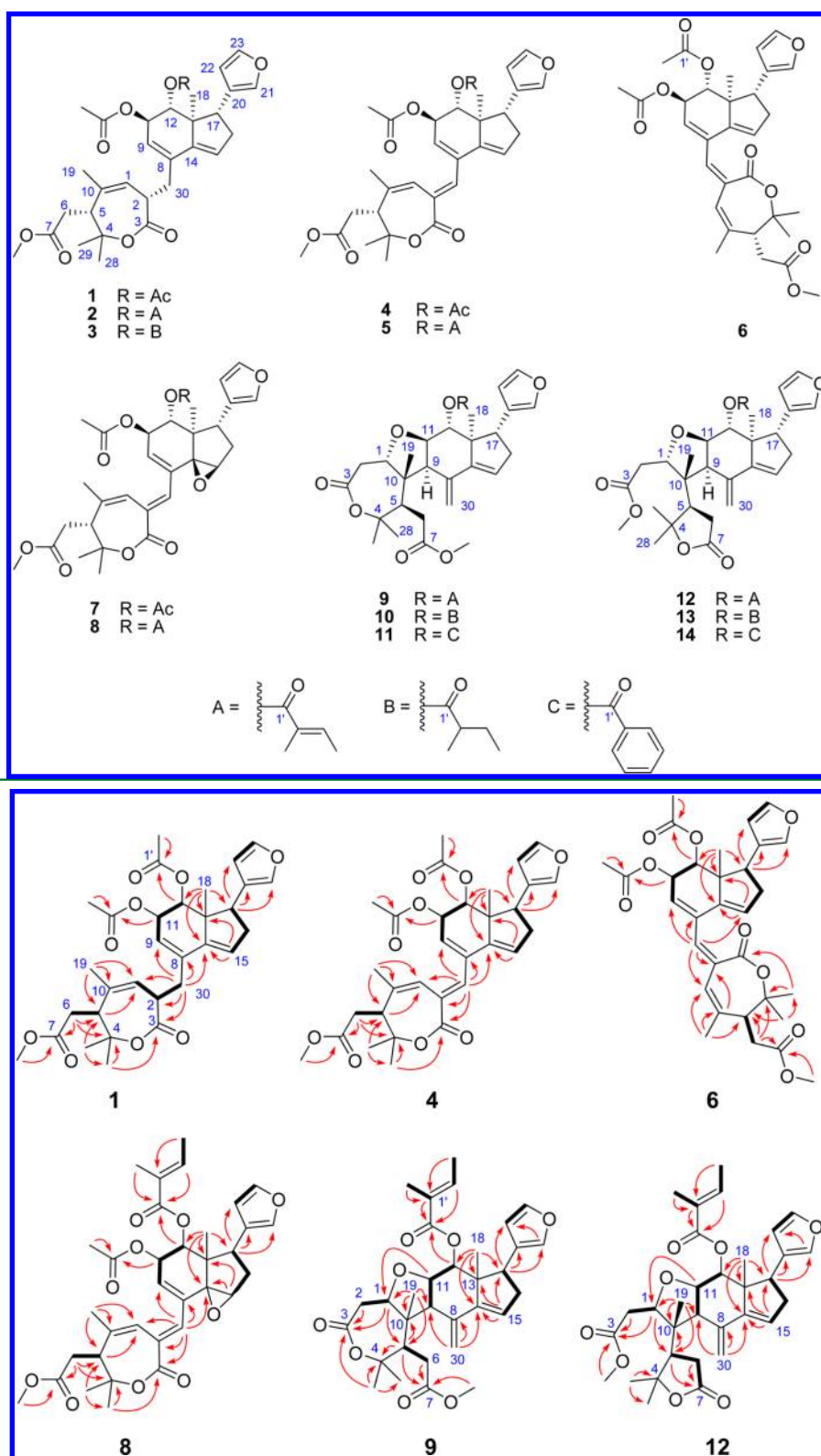


Figure 1. Key ^1H – ^1H COSY correlations (—) and HMBC correlations (→) of selected compounds.

The ^1H and ^{13}C NMR data (Table 1) of aphanamixoids D (2) and E (3) showed similar structural features to those of 1, except for the presence of a C-12 tigloyloxy group⁷ in 2 and a C-12 2-methylbutanoate group⁸ in 3, which were each confirmed by a HMBC cross-peak between H-12 and C-1' (Figure 1). The relative configurations of 2 and 3 were deduced

to be the same as 1 based on comparison of their NMR chemical shifts and ROESY correlations.

The ^1H and ^{13}C NMR data of aphanamixoid F (4) (Tables 2 and 3) were closely related to those of 1, except for replacement of an sp^3 C-2 methine signal and an sp^3 C-30 methylene signal with an sp^2 quaternary signal and an sp^2 methine signal in 4. The UV absorption at 291 nm indicated

Table 2. ^1H NMR Data for Compounds 4–8 in CDCl_3 (J in Hz)

position	4 ^a	5 ^a	6 ^a	7 ^b	8 ^a
1	6.09, s	6.19, s	5.94, s	6.14, s	6.18, s
5	2.76, br t (5.0)	2.83, dd (5.7, 4.9)	2.69, br t (5.1)	2.77, dd (5.8, 4.4)	2.79, dd (5.8, 4.4)
6a	2.88, dd (16.9, 5.6)	2.95, dd (16.9, 5.7)	2.88, dd (16.9, 5.9)	2.87, dd (17.0, 5.9)	2.90, dd (17.0, 5.8)
6b	2.29, dd (16.9, 4.6)	2.37, dd (16.9, 4.9)	2.25, dd (16.9, 4.4)	2.30, dd (17.0, 4.4)	2.32, dd (17.0, 4.4)
9	5.45, br s	5.92, br s	5.50, br s	5.87, br s	5.91, br s
11	5.68, d (8.2)	5.82, d (8.5)	5.58, d (8.2)	5.69, d (8.0)	5.78, d (8.0)
12	5.32, d (8.2)	5.48, d (8.5)	5.34, d (8.2)	5.59, d (8.0)	5.69, d (8.0)
15	5.84, br s	5.34, br s	5.70, br s	3.91, br s	3.94, br s
16 α	2.60, m	2.68, m	2.57, m	1.78, dd (14.0, 10.8)	1.82, dd (14.0, 10.8)
16 β				2.24, dd (14.0, 7.0)	2.26, dd (14.0, 7.0)
17	3.28, t (9.4)	3.38, dd (10.5, 8.5)	3.30, t (9.3)	3.01, dd (10.8, 7.0)	3.06, dd (10.8, 7.0)
18	1.06, s	1.16, s	1.05, s	1.05, s	1.10, s
19	1.90, s	1.97, s	1.89, s	1.92, s	1.94, s
21	7.22, s	7.18, s	7.20, s	7.15, s	7.07, s
22	6.30, br s	6.32, br s	6.30, br s	6.20, br s	6.18, br s
23	7.36, br s	7.36, br s	7.34, br s	7.34, br s	7.28, br s
28	1.42, s	1.49, s	1.40, s	1.40, s	1.44, s
29	1.54, s	1.62, s	1.61, s	1.52, s	1.55, s
30	7.09, s	7.18, s	6.34, s	6.52, s	6.57, s
7-OMe	3.71, s	3.78, s	3.70, s	3.71, s	3.74, s
11-O-Ac	2.05, s	2.09, s	2.04, s	2.07, s	2.07, s
12-O-2'	1.86, s		1.85, s	1.82, s	
12-O-3'		6.72, q (7.1)			6.61, q (7.1)
12-O-4'		1.81, d (7.1)			1.75, d (7.1)
12-O-5'		1.72, s			1.64, s

^aRecorded at 400 MHz. ^bRecorded at 600 MHz.

the presence of an extended conjugated system in **4** when compared to **1**. The absence of a ^1H – ^1H COSY correlation of H-1 and H-2 and the observed HMBC correlations [H-30 (δ_{H} 7.09)/C-1 (δ_{C} 118.1, CH), C-2 (δ_{C} 140.0, C), and C-3 (δ_{C} 168.3, C)] (Figure 1) confirmed the additional C-2–C-30 olefinic bond. The ROESY correlations (Figure S1, Supporting Information) of H-30/H-15 and H-9/H-1 suggested an *E*-configuration for this olefinic bond. The ROESY correlation of H-17/H-12 indicated that H-17 and H-12 are β -oriented, whereas the correlation of H₃-18/H-11 suggested the α -orientation of Me-18 and H-11. The remaining part of the structure and the relative configuration of **4** were similar to those of **1**, as determined from the HMBC and ROESY spectra. Aphanamixoid G (**5**) showed closely comparable structural features to those of **4** based on the 1D- and 2D-NMR data (Tables 2 and 3), except for the replacement of an acetoxy group with a tigloyloxy group at C-12 in **5**, as confirmed by the HMBC correlation of H-12/C-1'.

A molecular formula of $\text{C}_{31}\text{H}_{36}\text{O}_9$ was also obtained for aphanamixoid H (**6**), and the ^1H and ^{13}C NMR data of **6** (Tables 2 and 3) were closely related to those of compound **4**. A difference observed for **6** was the upfield shift of H-30 to δ_{H} 6.34 ($\Delta\delta$ –0.75). The ROESY correlations (Figure S1, Supporting Information) of H-30/H-9 and H-30/H-1 as well as the lack of a ROESY cross-peak between H-9 and H-1 indicated a *Z*-configuration for the C-2–C-30 olefinic bond in **6**.

The ^1H and ^{13}C NMR data (Tables 2 and 3) of aphanamixoids I (**7**) and J (**8**) indicated their similar structural features to those of **4** and **5**. In particular, the NMR data showed the presence of a C-12 acetoxy group in **7** and a C-12 tigloyloxy group in **8**. Compounds **7** and **8** were characterized by having a 14,15-epoxide moiety. The chemical shifts of C-14

at δ_{C} 69.4 (69.3, C) and C-15 at δ_{C} 60.1 (59.9, CH) as well as the HMBC correlations (Figure 1) of H₂-16/C-15, H-17/C-15, H₃-18/C-14, H-9/C-14, and H-30/C-14 confirmed the occurrence of a 14,15-epoxide group in both **7** and **8**. The ROESY correlations (Figure S1, Supporting Information) of H-30/H-15 and H-9/H-1 confirmed the *E*-configuration for the C-2–C-30 olefinic bond. The 14,15-epoxide was assigned as β -oriented based on the chemical shifts of H-15, C-14, and C-15, which were nearly identical to literature values for several known compounds incorporating a 14,15-epoxide in β -orientation established by X-ray crystallographic analysis.⁹

Aphanamixoid K (**9**) was obtained as a colorless, amorphous powder. The molecular formula was deduced by HREIMS to be $\text{C}_{32}\text{H}_{40}\text{O}_8$. An IR absorption band at 1736 cm^{-1} , as well as ^{13}C NMR signals at δ 173.6, 170.3, and 167.7, revealed three ester carbonyl groups. The observation of signals for a β -substituted furan ring (δ_{H} 6.19, 7.10, 7.27; δ_{C} 111.1, 140.2, 142.1), a methoxy group (δ_{H} 3.76; δ_{C} 52.1), four tertiary methyl groups (δ_{H} 0.81, 1.19, 1.40, 1.45), and a characteristic exocyclic double bond (δ_{H} 5.12, 5.40) in the ^1H and ^{13}C NMR spectra suggested that **9** is a priurianin-type limonoid.¹⁰ The NMR data of **9** showed a close similarity to those of the reported compound, aphanamixoid B,⁵ except for replacement of an acetoxy group with a tigloyloxy group at C-12 in **9**. The structure of **9** was confirmed by 2D-NMR experiments (Figure 1). The relative configuration of **9** was determined from the ROESY data (Figure S1, Supporting Information). The ROESY correlations of H₃-29/H₃-19, H₃-19/H-1, H-1/H-12, H-12/H-17, and H-17/H-16 β (δ_{H} 2.62) indicated that Me-29, Me-19, H-1, H-12, and H-17 are all on the same side of the molecule. These were assigned arbitrarily with a β -orientation. In turn, the observed correlations for H₃-18/H-11, H-11/H-9, H-9/H-5, and H-5/

Table 3. ^{13}C NMR Data for Compounds 4–8 in CDCl_3

position	4 ^a	5 ^a	6 ^a	7 ^b	8 ^a
1	118.1, CH	118.2, CH	122.8, CH	118.2, CH	118.2, CH
2	140.0, C	140.4, C	139.96, C	141.4, C	141.1, C
3	168.3, C	168.4, C	165.9, C	168.6, C	168.1, C
4	81.3, C	81.1, C	81.1, C	81.4, C	81.1, C
5	49.1, CH	49.0, CH	49.0, CH	49.4, CH	49.4, CH
6	34.8, CH ₂	34.7, CH ₂	34.7, CH ₂	33.0, CH ₂	32.7, CH ₂
7	173.2, C	173.2, C	173.3, C	173.4, C	173.1, C
8	131.7, C	131.6, C	132.9, C	132.2, C	132.1, C
9	126.3, CH	126.5, CH	124.5, C	133.6, CH	133.6, CH
10	133.1, C	133.0, C	134.9, C	134.1, C	133.8, C
11	72.3, CH	72.4, CH	72.5, CH	72.9, CH	72.9, CH
12	78.1, CH	78.0, CH	78.5, CH	76.3, CH	76.1, CH
13	51.0, C	51.3, C	51.6, C	45.2, C	45.3, C
14	144.6, C	144.6, C	144.1, C	69.4, C	69.3, C
15	126.4, CH	126.3, CH	125.1, CH	60.1, CH	59.9, CH
16	38.4, CH ₂	38.2, CH ₂	38.4, CH ₂	34.5, CH ₂	34.7, CH ₂
17	45.4, CH	45.2, CH	45.4, CH	37.3, CH	37.2, CH
18	14.4, CH ₃	14.6, CH ₃	13.7, CH ₃	13.0, CH ₃	13.0, CH ₃
19	26.2, CH ₃	26.1, CH ₃	25.8, CH ₃	26.2, CH ₃	26.0, CH ₃
20	123.5, C	123.3, C	124.0, C	122.3, C	121.9, C
21	140.5, CH	140.3, CH	139.98, CH	140.5, CH	140.6, CH
22	111.1, CH	111.1, CH	111.2, C	111.5, CH	111.2, CH
23	142.4, CH	142.2, CH	142.3, CH	142.8, CH	142.3, CH
28	28.7, CH ₃	28.7, CH ₃	28.9, CH ₃	28.9, CH ₃	28.7, CH ₃
29	26.0, CH ₃	26.0, CH ₃	25.6, CH ₃	26.1, CH ₃	25.9, CH ₃
30	137.0, CH	138.1, CH	136.0, CH	133.4, CH	133.4, CH
7-OMe	52.2, CH ₃	52.2, CH ₃	52.2, CH ₃	52.5, CH ₃	52.1, CH ₃
11-O-Ac	170.81, C	170.9, C	171.0, C	171.1, C	170.8, C
	21.1, CH ₃	21.0, CH ₃	21.1, CH ₃	21.1, CH ₃	21.0, CH ₃
12-O-1'	170.79, C	167.6, C	170.8, C	170.7, C	167.2, C
12-O-2'	21.0, CH ₃	128.2, C	21.0, CH ₃	21.3, CH ₃	128.2, C
12-O-3'		137.0, CH			138.0, CH
12-O-4'		14.4, CH ₃			14.3, CH ₃
12-O-5'		11.7, CH ₃			11.6, CH ₃

^aRecorded at 100 MHz. ^bRecorded at 150 MHz.

H₃-28 suggested Me-18, H-11, H-9, H-5, and Me-28 as being α -oriented.

The ^1H and ^{13}C NMR data (Tables 4 and 5) of aphanamixoids L (10) and M (11) showed similar structural features to those of 9, except for 10 having a C-12 2-methylbutanoate group and 11 a C-12 benzoyloxy group.¹¹ These assignments were confirmed by the HMBC cross-peak for H-12/C-1' for each case. The relative configurations of 10 and 11 were assigned as being the same as for 9, based on comparison of their NMR chemical shifts and ROESY correlations. The absolute configurations of aphanamixoids K–M (9–11) were determined by the ECD exciton chirality method.¹² These three compounds showed similar ECD splitting patterns in the 200–239 nm region (Figure 2). The sign of the first Cotton effect (9: $\Delta\epsilon$ +0.88 at λ_{max} 236 nm; 10: $\Delta\epsilon$ +1.00 at λ_{max} 236 nm; 11: $\Delta\epsilon$ +1.76 at λ_{max} 239 nm) was positive, whereas the sign of the second Cotton effect (9: $\Delta\epsilon$ +0.46 at λ_{max} 200 nm; 10: $\Delta\epsilon$ +0.41 at λ_{max} 203 nm; 11: $\Delta\epsilon$ +0.49 at λ_{max} 206 nm) was negative. This indicated that these compounds all exhibit positive chirality, and the two coupling chromophores of the conjugated double bonds (Woodward's rule gave calculated 237 nm) and the furan ring (λ_{max} calculated 206 nm)¹³ displayed a right-handed helicity. Furthermore, the ECD spectra of 9–11 were in good agreement with that of the

reported compound, aphanamixoid B, for which the absolute configuration was assigned by quantum chemical calculations of its ORD values and ECD spectrum.⁵ Therefore, the absolute configurations of compounds 9–11 were assigned as depicted.

The ^1H and ^{13}C NMR data of aphanamixoid N (12) (Tables 4 and 5) were closely related to those of 9. The NMR resonances for C-1, C-2, C-4, C-5, C-7, and C-29 of compound 12 were shifted by $\Delta\delta_{\text{C}}$ +2.2, $\Delta\delta_{\text{C}}$ –2.4, $\Delta\delta_{\text{C}}$ +2.9, $\Delta\delta_{\text{C}}$ +1.9, $\Delta\delta_{\text{C}}$ +1.7, and $\Delta\delta_{\text{C}}$ –2.9 ppm, respectively, relative to those of 9. These observations indicated that ring A in 12 is different from the seven-membered lactone ring in 9. HMBC correlations from the methoxy group (δ_{H} 3.76), H-1 (δ_{H} 4.17), and H-2 (δ_{H} 2.43) to C-3 (δ_{C} 170.9) were consistent with the methoxy group being connected to C-3. HMBC correlations from H-5 (δ_{H} 2.28) and H-6 (δ_{H} 2.76) to C-7 (δ_{C} 175.3) (Figure 1) as well as the absence of an HMBC correlation of H₃-29/C-3 indicated that C-4, C-5, C-6, and C-7 form a five-membered lactone ring in 12.

The relative configuration of compound 12 was determined as being the same as that of compound 9, based on detailed analysis of the ROESY data. The ROESY correlations of H₃-29/H₃-19, H₃-19/H-1, H-1/H-12, H-12/H-17, and H-17/H-16 β (δ_{H} 2.67) indicated that Me-29, Me-19, H-1, H-12, and H-17 were all similarly oriented. These were assigned with β -

Table 4. ^1H NMR Data for Compounds 9–14 in CDCl_3 (J in Hz)

position	9 ^a	10 ^b	11 ^b	12 ^b	13 ^b	14 ^a
1	4.13, dd (7.3, 3.9)	4.05, dd (9.6, 6.3)	4.21, dd (10.7, 4.7)	4.17, dd (8.9, 4.3)	4.22, m	4.22, dd (9.4, 3.8)
2	2.86, m	2.84, m	2.85, m	2.43, m	2.39, m	2.43, m
5	2.90, dd (7.1, 3.7)	2.90, dd (6.6, 3.8)	2.91, dd (5.8, 3.6)	2.28, t (8.3)	2.29, ^c m	2.28, br t (8.2)
6a	3.08, dd (13.3, 3.7)	3.07, dd (16.9, 3.8)	3.08, dd (13.6, 3.6)	2.76, br d (8.3)	2.81, ^c m	2.75, ^c m
6b	2.43, dd (13.3, 7.1)	2.40, dd (16.9, 6.6)	2.42, dd (13.6, 5.8)			
9	3.07, d (9.7)	3.04, d (8.2)	3.10, d (8.7)	3.25, d (8.6)	3.20, d (9.1)	3.28, d (8.6)
11	4.16, t (9.7)	4.10, dd (9.6, 8.2)	4.26, dd (9.6, 8.7)	4.25, t (8.6)	4.19, dd (9.1, 8.2)	4.16, t (8.6)
12	5.43, d (9.7)	5.34, d (9.6)	5.61, d (9.6)	5.33, d (8.3)	5.26, d (8.2)	5.51, d (8.6)
15	5.76, br s	5.77, br s	5.80, br s	5.78, br s	5.80, br s	5.80, br s
16 α	2.41, ddd (16.5, 10.1, 3.0)	2.39, ddd (16.5, 10.5, 3.0)	2.44, ddd (16.0, 9.4, 2.4)	2.42, ddd (16.6, 9.4, 2.8)	2.40, ddd (16.2, 9.6, 2.9)	2.44, ddd (16.8, 8.7, 2.9)
16 β	2.62, ddd (16.5, 8.5, 3.0)	2.60, ddd (16.5, 8.3, 3.0)	2.66, ddd (16.0, 8.1, 2.4)	2.67, ddd (16.6, 8.6, 2.8)	2.66, ddd (16.2, 8.4, 2.9)	2.70, ddd (16.8, 9.3, 2.9)
17	3.32, dd (10.1, 8.5)	3.33, dd (10.5, 8.3)	3.40, br t (9.4)	3.39, br t (9.4)	3.41, br t (9.3)	3.46, br t (9.3)
18	0.81, s	0.82, s	0.90, s	0.78, s	0.80, s	0.87, s
19	1.19, s	1.17, s	1.23, s	1.13, s	1.14, s	1.16, s
21	7.10, s	7.18, s	7.03, s	7.09, s	7.18, s	7.01, s
22	6.19, br s	6.26, br s	6.12, br s	6.19, br s	6.26, br s	6.12, br s
23	7.27, br s	7.30, br s	7.11, br s	7.27, br s	7.31, br s	7.12, br s
28	1.40, s	1.40, s	1.41, s	1.47, s	1.47, s	1.47, s
29	1.45, s	1.45, s	1.46, s	1.56, s	1.58, s	1.56, s
30a	5.40, s	5.40, s	5.43, s	5.40, s	5.41, s	5.41, s
30b	5.12, s	5.12, s	5.16, s	5.18, s	5.07, s	5.10, s
3-OMe				3.70, s	3.68, s	3.66, s
7-OMe	3.76, s	3.75, s	3.76, s			
12-O-2'		2.25, m			2.27, m	
12-O-3'a	6.72, q (7.0)	1.56, m	7.88, d (7.6)	6.74, q (7.3)	1.57, ^c m	7.90, d (7.4)
12-O-3'b		1.33, m			1.35, m	
12-O-4'	1.76, d (7.0)	0.86, t (7.5)	7.40, t (7.6)	1.75, d (7.3)	0.86, t (7.4)	7.39, t (7.4)
12-O-5'	1.71, s	0.94, d (7.0)	7.54, t (7.6)	1.73, s	0.97, d (7.0)	7.52, t (7.4)

^aRecorded at 600 MHz. ^bRecorded at 400 MHz. ^cOverlapped signals assigned by ^1H – ^1H COSY, HSQC, and HMBC spectra without designating multiplicity.

orientation arbitrarily, whereas the correlations of H_3 -18/ H -11, H -11/ H -9, H -9/ H -5, and H -5/ H_3 -28 suggested that Me-18, H -11, H -9, H -5, and Me-28 are all α -oriented. In terms of their biogenetic origin, compounds 9 and 12 may be connected through a series of reactions that involve a core transesterification reaction, which does not change the relative configuration at C-5. Furthermore, the ROESY cross-peak between H -9 and H -5 supported the α -orientation assigned for H -5.

According to the NMR data, aphanamixoids O (13) and P (14) showed similar structural features to those of 12, except for 13 possessing a C-12 2-methylbutanoate group and 14 a C-12 benzoyloxy group. On the basis of comparison of their NMR chemical shifts and ROESY correlations (Figure S1, Supporting Information), the relative configurations of 13 and 14 were confirmed as being the same as that of 12. The absolute configurations of 12–14 were also determined by the ECD exciton chirality method. The ECD spectra of 12–14 showed similar ECD splitting patterns (Figure 2), i.e., a positive first Cotton effect (12: $\Delta\epsilon$ +2.53 at λ_{max} 234 nm; 13: $\Delta\epsilon$ +0.54 at λ_{max} 237 nm; 14: $\Delta\epsilon$ +1.89 at λ_{max} 237 nm) and a negative second Cotton effect (12: $\Delta\epsilon$ +0.94 at λ_{max} 200 nm; 13: $\Delta\epsilon$ +0.29 at λ_{max} 204 nm; 14: $\Delta\epsilon$ +0.83 at λ_{max} 206 nm). These observations were consistent with the transition interaction between the two different chromophores of the conjugated double bonds (Woodward's rule gave calculated 237 nm) and the furan ring (λ_{max} calculated 206 nm).¹³ The clockwise

orientation of the two chromophores in space was used to establish the absolute configurations of 12–14, as shown.

In addition to the 14 new limonoids, 10 known terpenoids, piscidinol B,¹⁴ 25-methoxymogrol,¹⁵ turrapubesol B,¹⁶ rhoip-telic acid,¹⁷ ursolic acid,¹⁸ oleanolic acid,¹⁸ morolic acid,¹⁹ 15-hydroxy- α -cadinol,²⁰ 1S,4S,5S,10R-4,10-guaianediol,²¹ and 4(15)-eudesmene-1 β ,6 α -diol,²² were identified by comparing their spectroscopic data with those reported in the literature.

Antifeedant Activity of Compounds. Limonoids 1–14 were evaluated for their antifeedant activity against the cotton bollworm (*Helicoverpa armigera*). The results indicated that all of the compounds, except 6, showed antifeedant activity at the various concentration levels used. In particular, compounds 1, 4, and 5 exhibited potent antifeedant activity (Figures 3 and 4), with EC_{50} values of 0.017, 0.008, and 0.012 $\mu\text{mol}/\text{cm}^2$, respectively (Table S1, Supporting Information). Compounds 3, 8, and 9–14 were less active as antifeedants against *H. armigera*, with antifeedant indices from 11.11% to 47.31% at 2000 ppm (Figure 5; Table S2, Supporting Information). These results indicate that the aphanamixoids exhibit good antifeedant activities and may play a potent defensive role against herbivores in their plant of origin.

Structurally, the aphanamixoid-type limonoids (1–8) are quite similar, so a preliminary structure–activity relationship study was possible. Comparison of the EC_{50} values of 1 (0.017 $\mu\text{mol}/\text{cm}^2$) with 4 (0.008 $\mu\text{mol}/\text{cm}^2$) (Figure S2A, Supporting Information) and of 2 (0.049 $\mu\text{mol}/\text{cm}^2$) with 5 (0.012 $\mu\text{mol}/\text{cm}^2$) (Figure S2B, Supporting Information) indicated that

Table 5. ^{13}C NMR Data for Compounds 9–14 in CDCl_3

position	9 ^a	10 ^b	11 ^b	12 ^b	13 ^b	14 ^a
1	81.6, CH	81.6, CH	81.6, CH	83.8, CH	83.7, CH	84.1, CH
2	38.3, CH ₂	38.2, CH ₂	38.2, CH ₂	35.9, CH ₂	36.2, CH ₂	36.1, CH ₂
3	170.3, C	170.5, C	170.5, C	170.9, C	170.9, C	171.2, C
4	84.7, C	84.9, C	84.8, C	87.6, C	87.7, C	87.9, C
5	48.8, CH	48.6, CH	48.6, CH	50.7, CH	50.7, CH	51.0, CH
6	33.5, CH ₂	33.3, CH ₂	33.4, CH ₂	32.9, CH ₂	32.8, CH ₂	33.2, CH ₂
7	173.6, C	173.7, C	173.7, C	175.3, C	175.5, C	175.6, C
8	140.6, C	140.3, C	140.3, C	139.7, C	139.6, C	139.9, C
9	55.7, CH	55.6, CH	55.6, CH	49.4, CH	50.6, CH	50.1, CH
10	50.6, C	50.5, C	50.6, C	49.7, C	49.7, C	49.7, C
11	79.5, CH	79.6, CH	79.4, CH	79.6, CH	79.4, CH	79.7, CH
12	75.8, CH	75.3, CH	76.5, CH	79.0, CH	79.5, CH	80.1, CH
13	52.0, C	51.7, C	52.0, C	52.1, C	52.0, C	52.5, C
14	149.6, C	149.5, C	149.3, C	148.4, C	148.4, C	148.4, C
15	122.8, CH	123.1, CH	123.0, CH	122.9, CH	123.1, CH	123.4, CH
16	37.6, CH ₂	37.9, CH ₂	37.6, CH ₂	37.8, CH ₂	38.2, CH ₂	38.1, CH ₂
17	47.1, CH	47.4, CH	47.1, CH	45.6, CH	46.1, CH	45.9, CH
18	15.2, CH ₃	15.2, CH ₃	15.4, CH ₃	15.9, CH ₃	15.9, CH ₃	16.3, CH ₃
19	20.3, CH ₃	20.3, CH ₃	20.4, CH ₃	19.9, CH ₃	19.2, CH ₃	20.0, CH ₃
20	124.2, C	124.2, C	124.0, C	124.5, C	124.6, C	124.6, C
21	140.2, CH	140.0, CH	140.0, CH	140.0, CH	140.0, CH	140.2, CH
22	111.1, CH	111.2, CH	111.1, CH	111.0, CH	111.1, CH	111.2, CH
23	142.1, CH	142.3, CH	142.2, CH	142.2, CH	142.3, CH	142.5, CH
28	30.6, CH ₃	30.5, CH ₃	30.6, CH ₃	31.2, CH ₃	31.2, CH ₃	31.4, CH ₃
29	27.7, CH ₃	27.7, CH ₃	27.7, CH ₃	24.8, CH ₃	24.8, CH ₃	25.1, CH ₃
30	118.5, CH ₂	118.7, CH ₂	118.8, CH ₂	119.1, CH ₂	119.6, CH ₂	119.5, CH ₂
3-OMe				52.1, CH ₃	52.0, CH ₃	52.4, CH ₃
7-OMe	52.1, CH ₃	52.3, CH ₃	52.3, CH ₃			
12-O-1'	167.7, C	175.9, C	166.3, C	167.5, C	175.7, C	166.4, C
12-O-2'	128.6, C	41.6, CH	130.1, C	128.5, C	41.6, CH	130.5, C
12-O-3'	137.7, CH	26.4, CH ₂	129.7, CH	137.6, CH	26.4, CH ₂	129.9, CH
12-O-4'	14.3, CH ₃	11.6, CH ₃	128.2, CH	14.4, CH ₃	11.5, CH ₃	128.5, CH
12-O-5'	11.9, CH ₃	16.2, CH ₃	132.9, CH	12.0, CH ₃	16.2, CH ₃	133.2, CH

^aRecorded at 150 MHz. ^bRecorded at 100 MHz.

reduction of the C-2–C-30 olefinic bond affects the conjugated system of the compounds and reduces the resultant antifeedant activity. Furthermore, it was observed that compound **4**, with an *E*-configuration for this olefinic bond, more potently deterred *H. armigera* than compound **6**, which had a *Z*-configuration for this olefinic bond. Thus, it seems that the $\Delta^{2,30}$ configuration is vital to the antifeedant activity of these compounds. In addition, it can be inferred from the respective comparisons among compounds **1**, **2**, and **3**, **4** and **5**, and **7** and **8** that the acetoxy substituent at C-12 may improve the defensive effects of *H. armigera* (Figure S2C and D, Supporting Information).

Cytotoxicity Activities. Limonoids **1–14** were evaluated for their cytotoxicity against five human cancer cell lines, HL-60 (human promyelocytic leukemia cell line), SMMC-7721 (human hepatocellular carcinoma cell), A-549 (human lung cancer cell line), MCF-7 (human breast cancer cell line), and SW480 (colorectal cancer cell line), using the MTT method. However, none of these compounds showed cytotoxicity against any of the cell lines used ($\text{IC}_{50} > 10 \mu\text{M}$).

EXPERIMENTAL SECTION

General Experimental Procedures. Optical rotations were measured with a Perkin-Elmer model 241 polarimeter. UV spectroscopic data were obtained on a Shimadzu-210A double-beam

spectrophotometer. IR spectra were recorded on a Bruker-Tensor-27 spectrometer with KBr disks. ECD spectra were recorded with an Applied Photophysics Chirascan spectrometer. NMR experiments were carried out on a Bruker AM-400, Bruker DRX-500, or Avance III 600 NMR spectrometer. Chemical shifts were calculated using TMS as the internal standard. ESI and high-resolution mass spectra were recorded using a Finnigan MAT 90 instrument and VG Auto Spec-3000 spectrometer, respectively. Column chromatography (CC) was performed on silica gel (60–80 mesh, 200–300 mesh, 300–400 mesh, Qingdao Haiyang Chemical Co. Ltd., Qingdao, People's Republic of China), MCI gel (CHP20P, 75–150 μm , Mitsubishi Chemical Industries Ltd., Tokyo, Japan), C₈ reversed-phase silica gel (20–45 μm , Merck, Darmstadt, Germany), C₁₈ reversed-phase silica gel (40–63 μm , Merck, Darmstadt, Germany), or Sephadex LH-20 gel (40–70 μm , Amersham Pharmacia Biotech AB, Uppsala, Sweden). Precoated silica gel GF₂₅₄ plates (Qingdao Haiyang Chemical Plant) and precoated silica gel 60 F₂₅₄ (Merck) were used for TLC. Semi-preparative HPLC was performed on a Hypersil Gold RP-C₁₈ column (i.d. 10 \times 250 mm; Thermo Fisher Scientific Inc., Waltham, MA, USA) developed with CH₃CN/H₂O at room temperature.

Plant Material. Leaves and twigs of *A. polystachya* were collected at Lancang in Yunnan Province, People's Republic of China, in August 2011. The sample was identified by Mr. Yu Cheng, Kunming Institute of Botany, Chinese Academy Sciences (CAS). A voucher specimen (H20110821) was deposited at the State Key Laboratory of Phytochemistry and Plant Resources in West China, Kunming Institute of Botany, CAS.

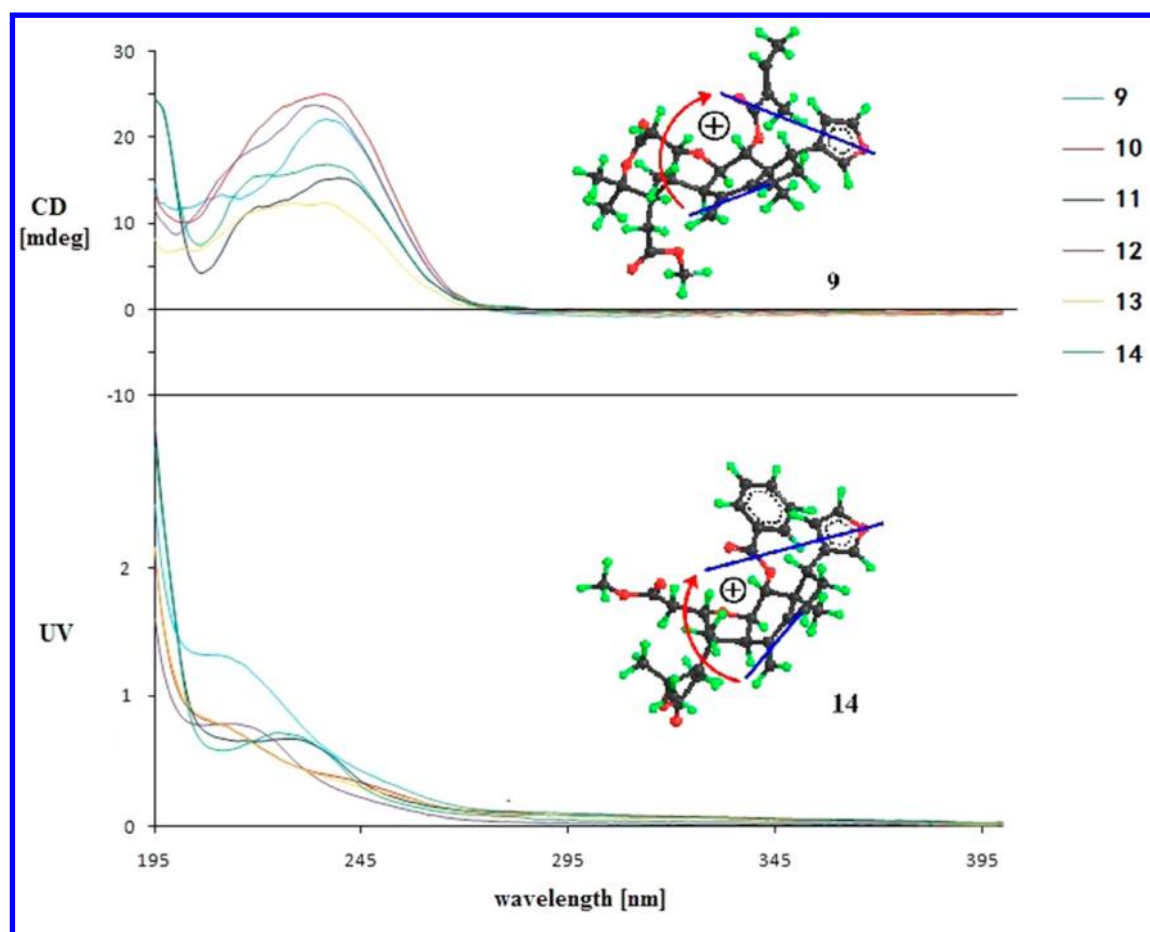


Figure 2. ECD and UV spectra of compounds 9–14. Bold lines denote the electric transition dipole of the chromophores in 9 and 14, respectively.

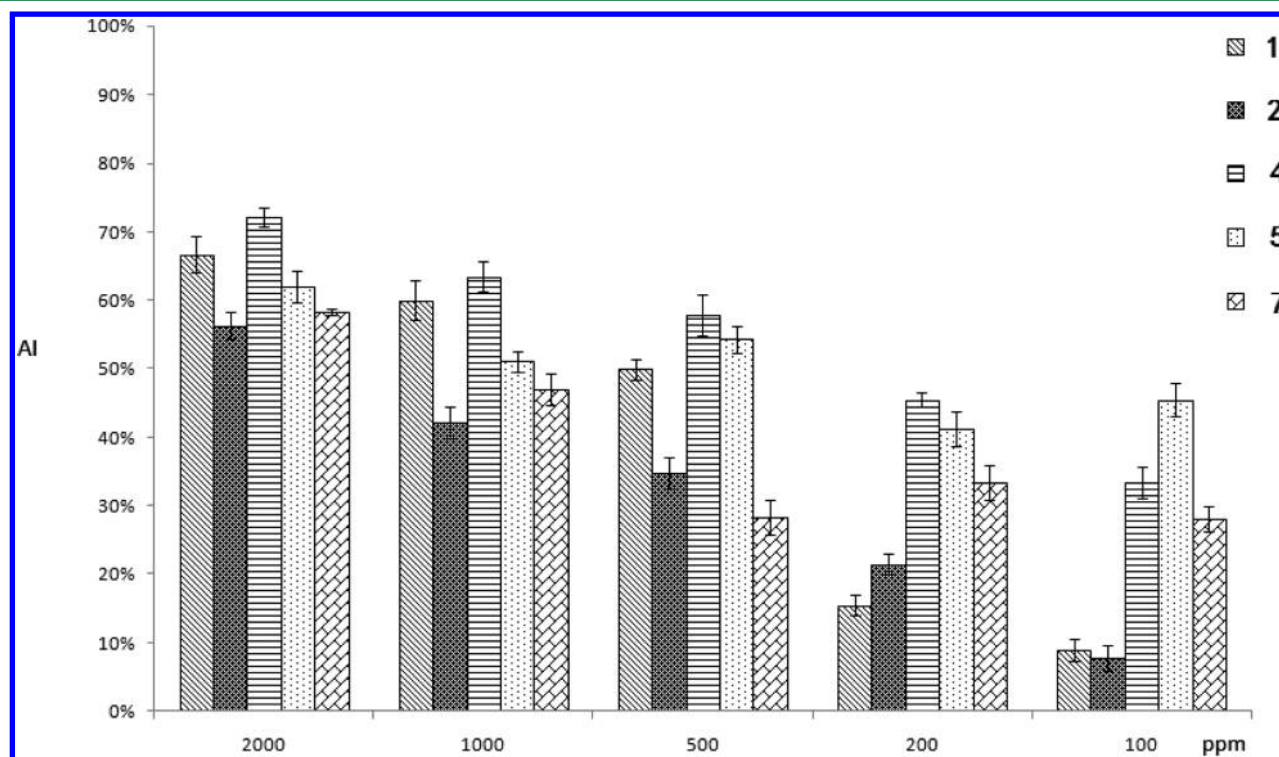


Figure 3. Antifeedant indices (AI) of compounds 1, 2, 4, 5, and 7 at concentrations of 100, 200, 500, 1000, and 2000 ppm.

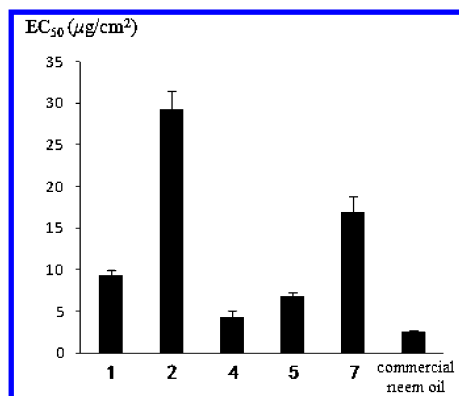


Figure 4. Antifeedant activities of compounds 1, 2, 4, 5, 7, and commercial neem oil.

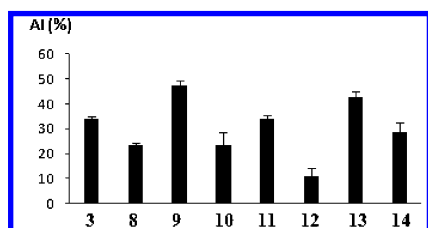


Figure 5. Antifeedant indices (AI) of selected compounds at 2000 ppm.

Extraction and Isolation. The leaves and twigs of *A. polystachya* (27 kg) were air-dried, powdered, and extracted three times with 90% ethanol. Evaporation of the solvent (under a vacuum) yielded a residue, which was suspended in water and then extracted successively with petroleum ether and ethyl acetate (EtOAc). The EtOAc extract (500 g) was subjected to passage over a silica gel column, which was eluted with mixtures of petroleum ether/acetone at a 2–50% gradient and of CHCl₃/MeOH at a 10–100% gradient, providing seven major pooled fractions. Fraction 3 (50 g) was separated on a column of MCI gel with a 30–100% MeOH/H₂O gradient, affording nine fractions (Fr. 3A–3I), and then fraction 3E was separated on a C₈ reversed-phase silica gel column with a 50–100% MeOH/H₂O gradient, yielding nine subfractions (Fr. 3E1–3E9). Fraction 3E2 was chromatographed on a C₁₈ column (eluted with 50–100% MeOH/H₂O), and then the fraction eluted with 60% MeOH (fraction 3E2A) was chromatographed on columns of Sephadex LH-20 (eluted with CHCl₃/MeOH), Sephadex LH-20 (eluted with acetone), and silica gel (eluted with 5% petroleum ether/EtOAc), to afford 7 (3 mg). Fraction 3E3 was chromatographed on a C₁₈ column (eluted with 50–100% MeOH/H₂O), and then the fraction eluted with 65% MeOH (fraction 3E3A) was chromatographed on columns of Sephadex LH-20 (eluted with CHCl₃/MeOH), Sephadex LH-20 (eluted with acetone), and silica gel (eluted with 5% petroleum ether/EtOAc), to afford two fractions, with each being further purified by semipreparative RP HPLC (eluted with 39–42% MeCN/H₂O), to afford 1 (12 mg), 4 (8 mg), and 6 (4 mg). Fraction 3E4 was chromatographed on a C₁₈ column (eluted with 50–100% MeOH/H₂O), and then the fraction that eluted with 85% MeOH (fraction 3E4A) was chromatographed over Sephadex LH-20 (eluted with CHCl₃/MeOH), Sephadex LH-20 (eluted with acetone), and silica gel (eluted with 5% chloroform/EtOAc), affording four fractions (Fr. 3E4A1–3E4A4). Two of these (Fr. 3E4A2 and 3E4A3) were further purified by semipreparative RP HPLC, eluting with 43% MeCN/H₂O, to afford 2 (5 mg), 5 (39 mg), and 8 (11 mg). Fraction 3E6 was chromatographed over Sephadex LH-20 (eluted with CHCl₃/MeOH), silica gel (eluted with petroleum ether/EtOAc), and Sephadex LH-20 (eluted with acetone), to afford 3 (2 mg) and 10 (10 mg). Fraction 4 (46 g) was separated on a column of MCI gel using a 30–100% MeOH/H₂O gradient, to afford seven fractions (Fr. 4A–4G). Fraction 4C was then separated on a column of

C₁₈ reversed-phase silica gel with 50–100% MeOH/H₂O, to afford nine subfractions (Fr. 4C1–3E9). Fraction 4C2 was chromatographed on columns of Sephadex LH-20 (eluted with CHCl₃/MeOH), silica gel (eluted with 10% petroleum ether/EtOAc), and silica gel (eluted with 12% petroleum ether/acetone), to afford 12 (14 mg) and 14 (10 mg). Fraction 4C4 was chromatographed on columns of Sephadex LH-20 (eluted with MeOH) and silica gel (eluted with 10% petroleum ether/acetone), to afford two fractions, 4C4B3 and 4C4B4. Fraction 4C4B3 was chromatographed on a column of Sephadex LH-20 (eluted with MeOH), to afford 9 (6 mg); fraction 4C4B4 was chromatographed on a column of Sephadex LH-20 (eluted with acetone), to afford 11 (10 mg). Fraction 4D5 was chromatographed on columns of Sephadex LH-20 (eluted with CHCl₃/MeOH), silica gel (eluted with 7% petroleum ether/EtOAc), and silica gel (eluted with 2% chloroform/EtOAc), to afford 13 (5 mg).

Aphanamixoid C (1): colorless, amorphous powder; $[\alpha]_D^{24}$ –45.9 (c 0.15, MeOH); UV (MeOH) λ_{\max} (log ϵ) 244 (3.24), 204 (3.34) nm; ECD (0.001 083 M, MeOH) λ_{\max} ($\Delta\epsilon$) 246 (–0.25), 219 (+0.31); IR (KBr) ν_{\max} 1743, 1738, 1640, 1630, 1378, 1246 cm^{–1}; ¹H and ¹³C NMR data, see Table 1; positive HREIMS $[M]^+$ m/z 554.2524 (calcd for C₃₁H₃₈O₉, 554.2516).

Aphanamixoid D (2): colorless, amorphous powder; $[\alpha]_D^{24}$ –47.9 (c 0.10, MeOH); UV (MeOH) λ_{\max} (log ϵ) 209 (3.61) nm; ECD (0.000 404 M, MeOH) λ_{\max} ($\Delta\epsilon$) 239 (+0.03), 221 (–0.36), 207 (–0.30); IR (KBr) ν_{\max} 1741, 1631, 1380, 1261, 1234 cm^{–1}; ¹H and ¹³C NMR data, see Table 1; positive HREIMS $[M]^+$ m/z 594.2830 (calcd for C₃₄H₄₂O₉, 594.2829).

Aphanamixoid E (3): colorless, amorphous powder; $[\alpha]_D^{25}$ –32.8 (c 0.15, MeOH); UV (MeOH) λ_{\max} (log ϵ) 205 (3.17) nm; ECD (0.001 006 M, MeOH) λ_{\max} ($\Delta\epsilon$) 246 (–0.08), 223 (–0.01); IR (KBr) ν_{\max} 2970, 2933, 1739, 1639, 1631, 1377, 1237 cm^{–1}; ¹H and ¹³C NMR data, see Table 1; positive HREIMS $[M]^+$ m/z 596.2966 (calcd for C₃₄H₃₃O₉, 596.2985).

Aphanamixoid F (4): colorless, amorphous powder; $[\alpha]_D^{25}$ –119.9 (c 0.21, MeOH); UV (MeOH) λ_{\max} (log ϵ) 292 (2.88), 243 (3.26), 216 (3.32) nm; ECD (0.000 57 M, MeOH) λ_{\max} ($\Delta\epsilon$) 237 (–1.39); IR (KBr) ν_{\max} 1744, 1729, 1710, 1691, 1641, 1631, 1378, 1245 cm^{–1}; ¹H and ¹³C NMR data, see Tables 2 and 3; positive HREIMS $[M]^+$ m/z 552.2365 (calcd for C₃₁H₃₆O₉, 552.2359).

Aphanamixoid G (5): colorless, amorphous powder; $[\alpha]_D^{24}$ –122.1 (c 0.23, MeOH); UV (MeOH) λ_{\max} (log ϵ) 290 (2.99), 215 (3.57) nm; ECD (0.000 583 M, MeOH) λ_{\max} ($\Delta\epsilon$) 231 (–1.18); IR (KBr) ν_{\max} 2924, 1737, 1707, 1631, 1384, 1260, 1025 cm^{–1}; ¹H and ¹³C NMR data, see Tables 2 and 3; positive HREIMS $[M]^+$ m/z 592.2676 (calcd for C₃₄H₄₀O₉, 592.2672).

Aphanamixoid H (6): colorless, amorphous powder; $[\alpha]_D^{25}$ –69.4 (c 0.13, MeOH); UV (MeOH) λ_{\max} (log ϵ) 285 (1.96), 213 (2.37) nm; ECD (0.001 177 M, MeOH) λ_{\max} ($\Delta\epsilon$) 243 (–0.49); IR (KBr) ν_{\max} 1744, 1728, 1711, 1690, 1640, 1631, 1375, 1245 cm^{–1}; ¹H and ¹³C NMR data, see Tables 2 and 3; positive HREIMS $[M]^+$ m/z 552.2365 (calcd for C₃₁H₃₆O₉, 552.2359).

Aphanamixoid I (7): colorless, amorphous powder; $[\alpha]_D^{25}$ –94.0 (c 0.10, MeOH); UV (MeOH) λ_{\max} (log ϵ) 284 (2.80), 207 (3.29) nm; ECD (0.001 109 M, MeOH) λ_{\max} ($\Delta\epsilon$) 277 (–0.17), 227 (–0.56); IR (KBr) ν_{\max} 2955, 2927, 1743, 1641, 1376, 1241, 1028 cm^{–1}; ¹H and ¹³C NMR data, see Tables 2 and 3; positive HREIMS $[M]^+$ m/z 568.2305 (calcd for C₃₁H₃₆O₁₀, 568.2308).

Aphanamixoid J (8): colorless, amorphous powder; $[\alpha]_D^{25}$ –159.6 (c 0.17, MeOH); UV (MeOH) λ_{\max} (log ϵ) 299 (3.06), 215 (3.55) nm; ECD (0.000 559 M, MeOH) λ_{\max} ($\Delta\epsilon$) 276 (–0.45), 223 (–1.47); IR (KBr) ν_{\max} 2958, 2924, 1743, 1710, 1640, 1630, 1378, 1055 cm^{–1}; ¹H and ¹³C NMR data, see Tables 2 and 3; positive HREIMS $[M]^+$ m/z 608.2615 (calcd for C₃₄H₄₀O₁₀, 608.2621).

Aphanamixoid K (9): colorless, amorphous powder; $[\alpha]_D^{29}$ +19.8 (c 0.14, MeOH); UV (MeOH) λ_{\max} (log ϵ) 213 (3.32) nm; ECD (0.000 76 M, MeOH) λ_{\max} ($\Delta\epsilon$) 236 (+0.88), 200 (+0.46); IR (KBr) ν_{\max} 2949, 2926, 1736, 1637, 1627, 1630, 1381, 1262, 1207, 1122 cm^{–1}; ¹H and ¹³C NMR data, see Tables 4 and 5; positive HREIMS $[M]^+$ m/z 552.2709 (calcd for C₃₂H₄₀O₈, 552.2723).

Aphanamixoid L (10): colorless, amorphous powder; $[\alpha]_D^{29} +23.4$ (c 0.12, MeOH); UV (MeOH) λ_{\max} (log ϵ) 373 (1.14), 210 (3.00) nm; ECD (0.000 758 M, MeOH) λ_{\max} ($\Delta\epsilon$) 236 (+1.00), 203 (+0.41); IR (KBr) ν_{\max} 2956, 2926, 1736, 1629, 1461, 1382, 1263, 1205, 1122 cm^{-1} ; ^1H and ^{13}C NMR data, see Tables 4 and 5; positive HREIMS $[\text{M}]^+ m/z$ 554.2892 (calcd for $\text{C}_{32}\text{H}_{43}\text{O}_8$, 554.2880).

Aphanamixoid M (11): colorless, amorphous powder; $[\alpha]_D^{28} +70.2$ (c 0.30, MeOH); UV (MeOH) λ_{\max} (log ϵ) 258 (2.72), 230 (3.45), 205 (3.17) nm; ECD (0.000 261 M, MeOH) λ_{\max} ($\Delta\epsilon$) 239 (+1.76), 206 (+0.49); IR (KBr) ν_{\max} 2956, 2925, 1732, 1726, 1634, 1629, 1456, 1378, 1272, 1237 cm^{-1} ; ^1H and ^{13}C NMR data, see Tables 4 and 5; positive HREIMS $[\text{M}]^+ m/z$ 574.2571 (calcd for $\text{C}_{34}\text{H}_{38}\text{O}_8$, 574.2567).

Aphanamixoid N (12): colorless, amorphous powder; $[\alpha]_D^{15} +96.7$ (c 0.20, MeOH); UV (MeOH) λ_{\max} (log ϵ) 214 (3.56) nm; ECD (0.000 285 M, MeOH) λ_{\max} ($\Delta\epsilon$) 234 (+2.53), 200 (+0.94); IR (KBr) ν_{\max} 2957, 2925, 2852, 1768, 1745, 1709, 1579, 1438, 1266, 1135, 1072, 1027 cm^{-1} ; ^1H and ^{13}C NMR data, see Tables 4 and 5; positive HRESIMS $[\text{M} + \text{Na}]^+ m/z$ 575.2631 (calcd for $\text{C}_{32}\text{H}_{40}\text{O}_8\text{Na}$, 575.2620).

Aphanamixoid O (13): colorless, amorphous powder; $[\alpha]_D^{29} -7.3$ (c 0.11, MeOH); UV (MeOH) λ_{\max} (log ϵ) 207 (3.05) nm; ECD (0.000 695 M, MeOH) λ_{\max} ($\Delta\epsilon$) 237 (+0.54), 204 (+0.29); IR (KBr) ν_{\max} 2968, 2938, 1768, 1743, 1632, 1462, 1383, 1270, 1182, 1147, 1025, 1015 cm^{-1} ; ^1H and ^{13}C NMR data, see Tables 4 and 5; positive HREIMS $[\text{M}]^+ m/z$ 554.2889 (calcd for $\text{C}_{32}\text{H}_{42}\text{O}_8$, 554.2880).

Aphanamixoid P (14): colorless, amorphous powder; $[\alpha]_D^{15} +47.5$ (c 0.13, MeOH); UV (MeOH) λ_{\max} (log ϵ) 228 (3.57), 200 (3.59) nm; ECD (0.000 272 M, MeOH) λ_{\max} ($\Delta\epsilon$) 237 (+1.89), 206 (+0.83); IR (KBr) ν_{\max} 2956, 2926, 2854, 1736, 1721, 1629, 1450, 1272, 1112, 1070, 1027 cm^{-1} ; ^1H and ^{13}C NMR data, see Tables 4 and 5; positive HRESIMS $[\text{M} + \text{H}]^+ m/z$ 575.2641 (calcd for $\text{C}_{34}\text{H}_{39}\text{O}_8$, 575.2644).

Antifeedant Activity Assay. A dual-choice bioassay²³ modified from a previous procedure²⁴ was performed as an antifeedant test. The insects, cotton bollworm (*Helicoverpa armigera*), were purchased from the Pilot-Scale Base of Bio-Pesticides, Institute of Zoology, Chinese Academy of Sciences. The larvae were reared on an artificial diet in the laboratory under a controlled photoperiod (light:dark, 12:8 h) and temperature (25 ± 2 °C). Larvae were starved 4–5 h prior to each bioassay. Fresh leaf disks were cut from *Brassica chinensis* L., using a cork borer (1.1 cm in diameter). Treated leaf disks were painted with 10 μL of acetone solution containing the test compound, and control leaf disks with the same amount of acetone. After air drying, two test leaf disks and two control ones were set in alternating position in the same Petri dish (90 mm in diameter), with a moistened filter paper at the bottom. Two-thirds of instars were placed at the center of the Petri dish. Five different concentrations of test compound (2000, 1000, 500, 200, 100 ppm) and a control were tested with five replicates per treatment. After feeding for 24 h, the areas of the leaf disks consumed were measured. The antifeedant index (AI) was calculated according to the formula

$$\text{AI} (\%) = [(C - T)/(C + T)] \times 100\%$$

where *C* and *T* represent the blank control and treated leaf areas consumed by the insect. The insect antifeedant potency of the test compound was evaluated in terms of the EC_{50} value (the effective concentration for 50% feeding reduction), which was determined by probit analysis for each insect species. A commercial neem oil product (with 1% azadirachtin) was used as positive control and was purchased from Kunming Rixin Dachuan Technology Co. Ltd. This was also evaluated for antifeedant activity as the method mentioned above.

Cytotoxicity Assay. Five human tumor cell lines (HL-60, SMMC-7721, A-549, MCF-7, and SW-480) were used. All cells were cultured in DMEM or RPMI-1640 medium (Hyclone, Logan, UT, USA) supplemented with 10% fetal bovine serum (Hyclone) at 37 °C in a humidified atmosphere with 5% CO_2 . Cell viability was assessed by conducting colorimetric measurements of the amount of insoluble formazan formed in living cells based on the reduction of 3-(4,5-dimethylthiazol-2-yl)-2,5-diphenyltetrazolium bromide (MTT) (Sigma, St. Louis, MO, USA). Briefly, 100 μL of adherent cells were

seeded into each well of a 96-well cell culture plate and allowed to adhere for 12 h before test compound addition, while suspended cells were seeded just before drug addition, both with an initial density of 5×10^3 to 1×10^4 cells/mL in 100 μL of medium. Each cell line was exposed to the test compound at 40 μM in triplicate for 48 h, with cisplatin and paclitaxel (Sigma) used as positive controls. After incubation, 20 μL of MTT (5 g/L) was added to each well, and the incubation continued for 4 h at 37 °C. The cells were next lysed with 200 μL of 10% sodium dodecyl sulfate after removing the medium. The optical density of the lysate was measured at 595 nm in a 96-well microtiter plate reader (Bio-Rad 680). The IC_{50} value of each compound was calculated using the method of Reed and Muench. Two positive controls, cisplatin and paclitaxel, were evaluated for their cytotoxicity against five human cancer cell lines. Cisplatin showed cytotoxicity with IC_{50} values of 1.8 μM for HL-60, 8.9 μM for SMMC-7721, 11.7 μM for A-549, 15.9 μM for MCF-7, and 16.7 μM for SW480. In turn, all the IC_{50} values of paclitaxel for the five human cancer cell lines were <0.008 μM .

■ ASSOCIATED CONTENT

§ Supporting Information

This material (^1H , ^{13}C NMR, DEPT, HSQC, HMBC, COSY, ROESY, ESI, HRMS, IR, ECD, and UV spectroscopic data for compounds 1–14, bioactivity assay data) is available free of charge via the Internet at <http://pubs.acs.org>.

■ AUTHOR INFORMATION

Corresponding Authors

* (S.-H. Li) E-mail: shli@mail.kib.ac.cn. Tel/Fax: (86) 871-65223035.

* (X.-J. Hao) E-mail: haoxj@mail.kib.ac.cn. Tel/Fax: (86) 871-65223070.

* (H.-P. He) E-mail: hehongping@mail.kib.ac.cn or hehongping@yahoo.com. Tel: (86) 871-65223263. Fax: (86) 871-65223070.

Notes

The authors declare no competing financial interest.

■ ACKNOWLEDGMENTS

This work was supported financially by the National Natural Science Foundation of China (30830114), the Ministry of Science and Technology (2009CB522300 and 2009CB940900), and the Candidates of the Young Academic and Technical Leaders of Yunnan Province (2010CI047). We thank Mr. Y. Cheng (Kunming Institute of Botany, CAS) for collection and identification of plant materials. We thank Prof. Y. Li (Kunming Institute of Botany, CAS) for bioactivity testing. We thank Dr. W.-G. Wang (Kunming Institute of Botany, CAS) for his valuable suggestions during the preparation of this article.

■ DEDICATION

Dedicated to Prof. Dr. Otto Sticher, of ETH-Zurich, Zurich, Switzerland, for his pioneering work in pharmacognosy and phytochemistry.

■ REFERENCES

- (1) Isman, M. B.; Koul, O.; Luczynski, A.; Kaminski, J. J. *Agric. Food Chem.* **1990**, *38*, 1406–1411.
- (2) (a) Simmonds, M. S. J.; Stevenson, P. C.; Porter, E. A.; Veitch, N. C. *J. Nat. Prod.* **2001**, *64*, 1117–1120. (b) Luo, X. D.; Wu, S. H.; Wu, D. G.; Ma, Y. B.; Qi, S. H. *Tetrahedron* **2002**, *58*, 7797–7804. (c) Nihei, K.-i.; Asaka, Y.; Mine, Y.; Yamada, Y.; Iigo, M.; Yanagisawa, T.; Kubo, I. *J. Nat. Prod.* **2006**, *69*, 975–977. (d) Fowles, R.; Mootoo, B.; Ramsewak, R.; Khan, A.; Ramsuhag, A.; Reynolds, W.; Nair, M.

- Pest Manage. Sci.* **2010**, *66*, 1298–1303. (e) Xu, H.; Zhang, J. L. *Bioorg. Med. Chem. Lett.* **2011**, *21*, 1974–1977. (f) Tan, Q. G.; Luo, X. D. *Chem. Rev.* **2011**, *111*, 7437–7522. (g) Fang, X.; Di, Y. T.; Hao, X. J. *Curr. Org. Chem.* **2011**, *15*, 1363–1391.
- (3) Yang, S. P.; Chen, H. D.; Liao, S. G.; Xie, B. J.; Miao, Z. H.; Yue, J. M. *Org. Lett.* **2011**, *13*, 150–153.
- (4) Zhang, Y.; Wang, J. S.; Wang, X. B.; Wei, D. D.; Luo, J. G.; Luo, J.; Yang, M. H.; Kong, L. Y. *Tetrahedron Lett.* **2011**, *52*, 2590–2593.
- (5) Cai, J. Y.; Zhang, Y.; Luo, S. H.; Chen, D. Z.; Tang, G. H.; Yuan, C. M.; Di, Y. T.; Li, S. H.; Hao, X. J.; He, H. P. *Org. Lett.* **2012**, *14*, 2524–2527.
- (6) (a) Kundu, A. B.; Ray, S.; Chatterjee, A. *Phytochemistry* **1985**, *24*, 2123–2125. (b) Mulholland, D. A.; Naidoo, N. *Phytochemistry* **1999**, *51*, 927–930. (c) Zhang, Y.; Wang, J. S.; Wang, X. B.; Gu, Y. C.; Wei, D. D.; Guo, C.; Yang, M. H.; Kong, L. Y. *J. Agric. Food Chem.* **2013**, *61*, 2171–2182.
- (7) (a) Najmuldeen, I. A.; Hadi, A. H. A.; Awang, K.; Mohamad, K.; Ketuly, K. A.; Mukhtar, M. R.; Chong, S. L.; Chan, G.; Nafiah, M. A.; Weng, N. S.; Shirota, O.; Hosoya, T.; Nugroho, A. E.; Morita, H. J. *Nat. Prod.* **2011**, *74*, 1313–1317. (b) Zhang, Q.; Di, Y. T.; He, H. P.; Fang, X.; Chen, D. L.; Yan, X. H.; Zhu, F.; Yang, T. Q.; Liu, L. L.; Hao, X. J. *J. Nat. Prod.* **2011**, *74*, 152–157. (c) Han, M. L.; Zhang, H.; Yang, S. P.; Yue, J. M. *Org. Lett.* **2012**, *14*, 486–489.
- (8) (a) Gan, L. S.; Wang, X. N.; Wu, Y.; Yue, J. M. *J. Nat. Prod.* **2007**, *70*, 1344–1347. (b) Li, M. Y.; Yang, X. B.; Pan, J. Y.; Feng, G.; Xiao, Q.; Sinkkonen, J.; Satyanandamurty, T.; Wu, J. *J. Nat. Prod.* **2009**, *72*, 2110–2114. (c) Ning, J.; Di, Y. T.; Zhang, X.; He, H. P.; Wang, Y. Y.; Li, Y.; Li, S. L.; Hao, X. J. *J. Nat. Prod.* **2010**, *73*, 1327–1331. (d) Li, J.; Li, M. Y.; Feng, G.; Zhang, J.; Karonen, M.; Sinkkonen, J.; Satyanandamurty, T.; Wu, J. *J. Nat. Prod.* **2012**, *75*, 1277–1283.
- (9) (a) Ndung'u, M.; Hassanali, A.; Hooper, A. M.; Chhabra, S.; Miller, T. A.; Paul, R. L.; Torto, B. *Phytochemistry (Elsevier)* **2003**, *64*, 817–823. (b) Mitsui, K.; Saito, H.; Yamamura, R.; Fukaya, H.; Hitotsuyanagi, Y.; Takeya, K. *J. Nat. Prod.* **2006**, *69*, 1310–1314.
- (10) (a) Lidert, Z.; Taylor, D. A. H.; Thirugnanam, M. J. *Nat. Prod.* **1985**, *48*, 843–845. (b) Sarker, S. D.; Savchenko, T.; Whiting, P.; Sik, V.; Dinan, L. *Arch. Insect Biochem. Physiol.* **1997**, *35*, 211–217. (c) Koul, O.; Daniewski, W. M.; Multani, J. S.; Gumulka, M.; Singh, G. *J. Agric. Food Chem.* **2003**, *51*, 7271–7275.
- (11) Chen, H. D.; Yang, S. P.; Liao, S. G.; Zhang, B.; Wu, Y.; Yue, J. M. *J. Nat. Prod.* **2008**, *71*, 93–97.
- (12) (a) Harada, N.; Nakanishi, K. *Acc. Chem. Res.* **1972**, *5*, 257–263. (b) Harada, N.; Uda, H. *J. Am. Chem. Soc.* **1978**, *100*, 8022–8024.
- (13) (a) Abdelgaleil, S. A. M.; Okamura, H.; Iwagawa, T.; Sato, A.; Miyahara, I.; Doe, M.; Nakatani, M. *Tetrahedron* **2001**, *57*, 119–126. (b) Lin, B. D.; Chen, H. D.; Liu, J.; Zhang, S.; Wu, Y.; Dong, L.; Yue, J. M. *Phytochemistry* **2010**, *71*, 1596–1601.
- (14) Govindachari, T. R.; Kumari, G. N. K.; Suresh, G. *Phytochemistry* **1995**, *39*, 167–170.
- (15) Chen, X. B.; Zhuang, J. J.; Liu, J. H.; Lei, M.; Ma, L.; Chen, J.; Shen, X.; Hu, L. H. *Bioorg. Med. Chem.* **2011**, *19*, 5776–5781.
- (16) Wang, X. N.; Fan, C. Q.; Yin, S.; Lin, L. P.; Ding, J.; Yue, J. M. *Helv. Chim. Acta* **2008**, *91*, 510–519.
- (17) Jiang, Z. H.; Zhou, R. H.; Masuda, K.; Ageta, H. *Phytochemistry* **1995**, *40*, 219–224.
- (18) Seebacher, W.; Simic, N.; Weis, R.; Saf, R.; Kunert, O. *Magn. Reson. Chem.* **2003**, *41*, 636–638.
- (19) Majumder, P. L.; Maiti, R. N.; Panda, S. K.; Mal, D. J. *Org. Chem.* **1979**, *44*, 2811–2812.
- (20) Kuo, Y. H.; Chen, C. H.; Chien, S. C.; Lin, Y. L. *J. Nat. Prod.* **2002**, *65*, 25–28.
- (21) Zhang, G. W.; Ma, X. Q.; Su, J. Y.; Zhang, K.; Kurihara, H.; Yao, X. S.; Zeng, L. M. *Nat. Prod. Res.* **2006**, *20*, 659–664.
- (22) (a) Kamel, A. J. *Nat. Prod.* **1995**, *58*, 428–431. (b) Sun, Z.; Chen, B.; Zhang, S.; Hu, C. J. *Nat. Prod.* **2004**, *67*, 1975–1979.
- (23) (a) Luo, S. H.; Luo, Q.; Niu, X. M.; Xie, M. J.; Zhao, X.; Schneider, B.; Gershenzon, J.; Li, S. H. *Angew. Chem., Int. Ed.* **2010**, *49*, 4471–4475. (b) Luo, S. H.; Weng, L. H.; Xie, M. J.; Li, X. N.; Hua, J.; Zhao, X.; Li, S. H. *Org. Lett.* **2011**, *13*, 1864–1867.
- (24) Solis, P. N.; Wright, C. W.; Anderson, M. M.; Gupta, M. P.; Phillipson, J. D. *Planta Med.* **1993**, *59*, 250–252.